

R-Spondin 2 signaling mediates susceptibility to fatal infectious diarrhea

Olivier Papapietro^{1,2}, Sarah Teatero^{1,2}, Ajitha Thanabalasuriar^{1,2}, Kyoko E. Yuki^{2,3}, Eduardo Diez^{1,2}, Lei Zhu^{1,2}, Eugene Kang^{1,2}, Sandeep Dhillon^{4,5,6}, Aleixo M. Muise^{4,5,6}, Yves Durocher⁷, Martin M. Marcinkiewicz⁸, Danielle Malo^{2,3,9}, and Samantha Gruenheid^{1,2}

¹Department of Microbiology and Immunology, McGill University, Montreal, QC, H3A 2B4, Canada

²Complex Traits Program, McGill University, Montreal, QC, H3G 0B1, Canada

³Department of Human Genetics, McGill University, Montreal, QC, H3A 1B1, Canada

⁴SickKids Inflammatory Bowel Disease Center and Cell Biology Program, Research Institute, Hospital for Sick Children, Toronto, ON, M5G 1X8, Canada

⁵Institute of Medical Science, University of Toronto, Toronto, ON, M5S 1A8, Canada

⁶Division of Gastroenterology, Hepatology, and Nutrition, Department of Pediatrics, University of Toronto, Hospital for Sick Children, Toronto, ON, M5G 1X8, Canada

⁷Biotechnology Research Institute, National Research Council of Canada, 6100 Royalmount Avenue, Montreal, QC, H4P 2R2, Canada

⁸Cytochem Inc., 6465 Durocher Avenue, Suite 400, Montreal, QC, H2V 3Z1, Canada

⁹Department of Medicine, McGill University Health Center, Montreal, QC, H3G 1Y6, Canada

Abstract

Citrobacter rodentium is a natural mouse pathogen widely used as a model for enteropathogenic and enterohemorrhagic *Escherichia coli* infections in humans. While *C. rodentium* causes self-limiting colitis in most inbred mouse strains, it induces fatal diarrhea in susceptible strains. The physiological pathways as well as the genetic determinants leading to susceptibility have remained largely uncharacterized. Here we use a forward genetic approach to identify the *R-spondin2* gene (*Rspo2*) as a major determinant of susceptibility to *C. rodentium* infection. Robust induction of *Rspo2* expression during infection in susceptible mouse strains causes a potent Wnt-mediated proliferative response of colonic crypt cells, leading to the generation of an immature and poorly differentiated colonic epithelium with deficiencies in ion-transport components. Our data demonstrate a previously unknown role of R spondins and Wnt signaling in susceptibility to

Users may view, print, copy, and download text and data-mine the content in such documents, for the purposes of academic research, subject always to the full Conditions of use:http://www.nature.com/authors/editorial_policies/license.html#terms

Correspondence: Samantha Gruenheid, Ph.D., samantha.gruenheid@mcgill.ca, Tel: 514-398-2138, Fax: 514-398-2603.

Supplementary Information is available.

Author Contributions: OP, ST, LZ, ED, AT, KY, EK, SD, YD and MMM performed experiments. OP, ST, ED, MMM, DM, AMM and SG designed the experiments and analyzed the data. OP and SG wrote the paper. All authors discussed the results and commented on the manuscript.

Conflict of interest statement: The authors declare no conflict of interest.

infectious diarrhea and identify *Rspo2* as a key molecular link between infection and intestinal homeostasis.

Introduction

Enteropathogenic *Escherichia coli* (EPEC) and enterohemorrhagic *Escherichia coli* (EHEC) are closely related human-specific diarrheal pathogens that are important causes of morbidity and mortality worldwide, especially in young children^{1,2}. EPEC and EHEC cause characteristic Attaching and Effacing (A/E) lesions in the infected intestine with tight attachment of bacteria to enterocytes, effacement of microvilli structures and profound remodeling of intestinal epithelium and mucosae^{3,4}. Despite evidence of variability in disease severity and clinical outcome of EPEC and EHEC infections^{5,6}, little is known about the mechanisms that regulate host susceptibility to these important pathogens. The mouse-specific pathogen *C. rodentium* is recognized as a good model for EPEC and EHEC⁷ and can be used to study the genes implicated in host response to A/E pathogens⁸. Following *C. rodentium* infection, the inbred strains C3H/HeJ⁸ (hereafter called C3), C3H/HeOJ⁹ (hereafter called C3Ou), and FVB¹⁰ display high levels of mortality while C57BL/6 (B6) mice develop self-limiting colitis⁹. Transcriptome analysis in total colonic samples from resistant or susceptible infected mice identified a common pathogenic mechanism in C3Ou and FVB mice that implicates decreased levels of expression of the major colonic HCO₃⁻/Cl⁻ exchanger *Slc26a3* and the carbonic anhydrase IV (*Car4*) together with fluid loss in feces and perturbations in electrolyte absorption¹¹. Accordingly, susceptible animals can be rescued by intensive fluid therapy¹². We previously reported a genome-wide search carried out in cohorts of F2 progeny of susceptible C3Ou or C3 and resistant B6 mice that led to the identification of a major genetic locus on chromosome 15 controlling mortality during *C. rodentium* infection, which we called *Cri1*¹³. Further genotype segregation analyses in F2 (B6 x FVB)¹⁴ populations implicate *Cri1* as the common genetic cause of susceptibility of C3, C3Ou and FVB mice. Generation of congenic mice with an introgressed segment of chromosome 15 from resistant B6 genome on the susceptible C3Ou genomic background (C3Ou.B6-*Cri1*) confirmed the effect of *Cri1* with full survival of congenic animals and revealed that susceptibility to *C. rodentium* infection was independent of the bacterial load carried by the host during disease¹³.

Here, we perform genetic, physical, bioinformatic and functional dissection of the *Cri1* locus and identify pathological *Rspo2*-mediated Wnt activation as a major contributor to mortality following *C. rodentium* infection in mice. R-spondins have been implicated in intestinal morphogenesis, proliferation and carcinogenesis: our data demonstrate a previously unknown role for these proteins in the response to intestinal infection.

Results

Cri1 mediates susceptibility of AKR/J and B6.C3Ou-*Cri1* mice

In addition to C3, C3Ou, and FVB mice, we noted that the AKR/J strain exhibited innate susceptibility to *C. rodentium* infection, with a mortality rate of 66% by day 30 post-infection (Supplementary Fig. S1). To assess whether susceptibility of AKR/J mice was

conferred by the *Cri1* locus, we generated an F2 (B6 x AKR/J) population, infected with *C. rodentium*, and monitored survival. Mice were genotyped at rs3683812, a SNP marker located at the peak of *Cri1*. Mice homozygous or heterozygous for AKR/J alleles at this marker suffered 63% and 58% mortality respectively, whereas mice homozygous for B6 alleles displayed 4% mortality, clearly demonstrating a role for *Cri1* in the susceptibility of AKR/J mice following *C. rodentium* infection (Supplementary Fig. S2). Thus, *Cri1* is the common genetic cause of susceptibility of the only four inbred mouse strains known to be hyper-susceptible to *C. rodentium* infection (C3, C3Ou, FVB, and AKR).

As described in the introduction, generation of congenic mice with an introgressed segment of chromosome 15 from resistant B6 genome on the susceptible C3Ou genomic background (C3Ou.B6-*Cri1*) confirmed the effect of *Cri1* with full survival of congenic animals. To test the effect of *Cri1* on the B6 background, we introgressed of a region of chromosome 15 containing *Cri1* from the susceptible C3Ou genome on the resistant B6 background (B6.C3Ou-*Cri1*). 45% of congenic animals succumbed to infection between days 13 and 28 post-infection (Supplementary Fig. S3a–b). Thus, despite modifying effects of the background genome, the genetic origin of *Cri1* is a major determinant of *C. rodentium* infection outcome.

Implication of *Rspo2* in *Cri1*-mediated susceptibility

Two sub-congenic lines, derived from resistant C3Ou.B6-*Cri1* congenic mice and characterized by recombinations within *Cri1*, were used to refine the localization of the *Cri1* locus (Fig 1a). Mice from the sub-congenic A line (congenic region 41.20 – 68.76 Mb.) were resistant to infection (100% survival 30 days post infection), whereas in the sub-congenic B line (congenic region 45.16–62.47 Mb), the introgression of segments from the resistant B6 genome had no effect on survival, leading to 92% mortality of this strain after 14 days of *C. rodentium* infection. These results unambiguously localize *Cri1* to a ~4 Mb interval (Fig 1a, b).

To identify the genetic determinant within this interval, we prioritized the region of overlap of the 95% confidence intervals defined by our previous genome wide analyses¹³ (Fig 1c). Haplotype analysis of this prioritized region identified a common and specific haplotype block shared by susceptible mice and absent from resistant mouse strains that encompasses only five genes: the proximal region of *Rspo2* (including the first two exons), *Eif3e*, *Gm10373*, *Ttc35* and *Tmem74* (Sup Fig 4). We performed sequencing analyses of these five prioritized candidate genes and found no coding differences between susceptible and resistant strains. Expression of all the candidate genes was determined by qPCR in colonic samples from susceptible C3Ou mice or resistant C3Ou.B6-*Cri1* mice left uninfected or at several time points after infection (Fig 1d). We found the *Rspo2* gene to be rapidly, strongly, and continuously induced during infection in susceptible C3Ou mice whereas no upregulation of *Rspo2* transcript was observed in resistant congenic mice. None of the other candidates were differentially regulated in C3Ou vs. C3Ou.B6-*Cri1* mice, nor were the genes *Angpt1*, *Abra* and *Oxr1*, which are located centromeric to *Rspo2*, outside of the prioritized haplotype, but still within the minimal interval delineated by genetic and physical mapping (Fig 1d). We further examined *Rspo2* expression during *C. rodentium* infection in resistant

B6 mice as well as in susceptible AKR and FVB mice and found that upregulation of *Rspo2* during infection is a common and specific feature of all mouse strains displaying *Cri1*-mediated susceptibility to *C. rodentium* infection (Fig 1e) including the B6.C3Ou-*Cri1* susceptible mice (Supplementary Fig. S3c).

***Rspo2* expression in colonic subepithelial stromal cells**

Rspo2 encodes a member of the R-Spondin family of secreted proteins (R-spondin 1-4) involved in β -catenin activation through the canonical Wnt pathway¹⁵. R-spondins were initially described as mitogens for epithelial cells of the mouse gastrointestinal tract^{15,16}. Recent work has revealed an important role for R-Spondin proteins in the maintenance of intestinal stem cells *in vitro* via their interaction with Lgr5 receptors¹⁷, and transcriptionally-activating gene fusions involving *RSPO2* and *RSPO3* have been found associated with 10% of colon tumours in humans¹⁸. However, the cellular source of R-Spondin and the mechanisms that regulate R-Spondin expression within the intestine remain largely uncharacterized.

To investigate the cellular source of *Rspo2* during *C. rodentium* infection, we performed reciprocal bone marrow chimera experiments with susceptible C3Ou and resistant C3Ou.B6-*Cri1* congenic mice. We found that the radio-resistant (non-hematopoietic) compartment conferred both mortality following infection and *Rspo2* induction in the chimeric mice (Fig 2a–b). This is consistent with previous work¹¹, suggesting that *Cri1*-mediated susceptibility is not associated with dysregulation of the immune response.

We next used *in situ* hybridization (ISH) on formalin-fixed, paraffin embedded (FFPE) colon sections from infected C3Ou and C3Ou.B6-*Cri1* mice to localize *Rspo2*-expressing cells. *Rspo2* expression was only readily detectable in infected susceptible C3Ou mice (Fig 3a) where evident labeling of cells within the Lamina Propria was observed (Fig 3b). Combined ISH and immunohistochemistry revealed that *Rspo2* transcripts were expressed in a cell population including α -smooth muscle actin (α -SMA)-positive intestinal myofibroblasts but excluding Gr1+ infiltrating neutrophils (Fig 3c–d). Together, these results provide evidence that during *C. rodentium* infection of susceptible mice, *Rspo2* expression is induced in subepithelial stromal cells, but not in intestinal epithelial cells or hematopoietic immune cells.

Activation of Wnt signaling in the colon of susceptible mice

Histological analysis of H&E stained FFPE sections showed a significant impact of the *Cri1* locus on the kinetics of *C. rodentium*-induced epithelial hyperplasia (Fig 4a). At 3 and 6 days post-infection, crypt lengths were significantly increased in C3Ou compared to C3Ou.B6-*Cri1* mice (Fig 4a). Using PCNA staining to monitor cellular proliferation, we also noted qualitative differences in epithelial proliferation (Fig 4b). By day 6 post-infection, proliferative cells were observed throughout the entire extent of the colonic epithelium in susceptible C3Ou mice with no non-proliferating differentiated compartment observable. In contrast, in resistant congenic mice, the boundary between the proliferative compartment and the differentiated epithelium was well-maintained and proliferation was delayed (Fig 4b).

Wnt signaling was strongly activated upon infection in susceptible mice but not in resistant mice. Although C3Ou and C3Ou.B6-*Cri1* mice had similar levels and membranous localization of β -catenin prior to infection, C3Ou mice displayed a striking cytoplasmic accumulation of total and activated β -catenin during infection which was not observed in C3Ou.B6-*Cri1* mice (Fig 4c–g). As further evidence of β -catenin activation, we found the Wnt target genes encoding c-Myc, cyclinD1 and the matrix metalloproteinase 7 to be specifically induced in susceptible animals (Fig 4h–j). Treatment of resistant congenic mice during *C. rodentium* infection with recombinant R-Spondin 2 protein induced β -catenin activation and a proliferative response as compared to control infected and BSA treated animals, and similar to what is observed in susceptible mice (Fig 4k). Overall, these observations demonstrate that *Cri1*-mediated susceptibility is associated with functional activation of Wnt signaling and a proliferative response, through *Rspo2* induction in infected mice.

Loss of intestinal differentiation in susceptible mice

Wnt/ β -catenin signaling has a key role in colon homeostasis, allowing maintenance of pluripotent colonic crypt stem cells and the continuous generation of undifferentiated transient amplifying precursors which differentiate as they migrate up the crypts. This gives rise to differentiated absorptive epithelial cells and goblet cells, which are continually sloughed off and replaced every three to four days in mice. Wnt signaling is normally restricted to the proliferative compartment that comprises the bottom third of the colonic crypts: as the cells reach the midcrypt region, Wnt signaling is downregulated to allow cell cycle arrest and differentiation¹⁹. Because strong Wnt signaling is known to inhibit colonic epithelial differentiation^{19,20}, and because loss of function of colonic epithelium has been proposed as a mechanism for *C. rodentium* susceptibility^{11,12}, we hypothesized that *Rspo2* induction in susceptible mice would lead to critical perturbations in the differentiation of the large intestinal epithelium. Indeed, a pronounced loss of colonic goblet cells was observed in susceptible animals, as indicated by Alcian blue staining (Fig 3a) and by qPCR analysis of markers of differentiated goblet cells (Fig 3b). Although there was a loss of goblet cells observed in resistant mice, it was minor and delayed compared to what was seen in susceptible mice (Fig 3a–b). The markers of terminally differentiated enterocytes *Slc26a3* and *Car4* were also found to be dramatically downregulated in susceptible mice (Fig 3c–d). *Slc26a3* (previously known as *Dra*: Down Regulated in Adenocarcinomas) encodes the major colonic $\text{Cl}^-/\text{HCO}_3^-$ exchanger which is exclusively expressed in differentiated enterocytes^{10,21,22}, and together with carbonic anhydrase IV (*Car4*) forms a functional unit for intestinal electroneutral absorption of chloride²³. Importantly, downregulation of *Car4* has been independently linked to lethality after *C. rodentium* infection^{11,12} and to excessive Wnt signaling in colonic crypts²⁰. Consistent with these works, we found a dramatic loss of *Car4* expression at the mRNA and protein levels, and a 1000 fold downregulation of *Slc26a3* transcript in infected susceptible C3Ou mice. The resistant congenic mice C3Ou.B6-*Cri1* maintained a significantly higher expression of *Slc26a3* and *Car4* than the parental C3Ou mice (Fig 3c–d). Mutations in *Slc26a3* in humans and mice cause congenital chloride-losing diarrhea^{24,25}, thus providing a link between the consequences of *Rspo2* induction and diarrheal disease.

To demonstrate a direct link between activation of Wnt signaling and *Cri1* mediated susceptibility to infection, we treated infected susceptible mice with recombinant DKK-1, a well-known antagonist of Wnt signaling. Notably, DKK-1 treatment decreased *C. rodentium*-induced β -catenin accumulation and activation (Fig 3e), increased levels of goblet cells (Fig 3f–g) and increased *Slc26a3* and *Car4* expression (Fig h–i) compared to mock-treated infected C3Ou mice. Daily DKK-1 treatment of susceptible mice throughout the course of infection significantly increased survival compared with mock-treated infected mice (40% vs 10% survival; mean survival time 15 days vs 11 days; P value < 0.04) (Fig 3j). Thus, inhibition of Wnt signalling through DKK-1 administration counterbalances the *C. rodentium*-induced Wnt activation in susceptible mice leading to longer survival in treated animals.

Discussion

Mouse forward genetics is a powerful tool for the identification of genes and pathways important in biological process and has been very valuable for the characterization of key players in bacterial sensing, early response to infection and intestinal inflammation^{26,27}. Here, we describe a single gene that naturally regulates susceptibility to enteric infection by *C. rodentium* in inbred mouse strains and uncover an unexpected link between bacterial sensing and intestinal homeostasis. Our data leads us to propose a model where *C. rodentium* induces mucosal *Rspo2* expression in susceptible mice, inducing proliferation of intestinal precursors and inhibiting differentiation of mature absorptive enterocytes and goblet cells, ultimately leading to the generation of a poorly differentiated epithelium and to fatal colitis (Fig 6).

We previously measured colon weights in susceptible and resistant congenic mice on day 9 of *C. rodentium* infection and concluded that *Cri1* did not impact intestinal hyperplasia at that time point¹³. However, data we present here directly measuring crypt heights and cellular phenotypes throughout the course of infection demonstrates that intestinal proliferation following *C. rodentium* infection is, in fact, kinetically and qualitatively distinct in resistant and susceptible mice. Furthermore, we hypothesize that it is not hyperplasia per se, but rather, the loss of differentiated intestinal function that ultimately leads to death in susceptible strains.

Genetic dissection of the *Cri1* locus allowed us to define a critical interval, containing *Rspo2*, that controls *C. rodentium* infection outcome. We also unambiguously associate mortality with upregulation of *Rspo2* expression. However, the mechanisms that regulate *Rspo2* expression in susceptible mice remain to be characterized. The minimal genetic interval for *Cri1* contains a haplotype block specific to susceptible mouse strains and containing the proximal region of *Rspo2* including the entire intergenic region between *Eif3e* and *Rspo2*. We hypothesize that the genetic difference(s) underlying *Rspo2* induction and susceptibility to infection localize to this region and confer differences in transcriptional regulation between resistant and susceptible mice. Identification of the specific genetic variations within this region that impact on *Rspo2* transcriptional regulation is an important subject for further studies and will provide additional corroboration of the underlying mechanism of susceptibility in these mice.

Tight regulation of the Wnt signaling pathway is critical to ensure normal function of the intestine, and maintaining a proper balance is key to intestinal health. Here we show that induction of robust Wnt signaling during intestinal infection is strongly correlated with mortality in susceptible mice. Conversely, stringent blockade of Wnt signaling through treatment of mice with a DKK1-expressing adenovirus markedly inhibited proliferation in the small intestine and colon, leading to progressive architectural degeneration, ulceration, and death²⁸. This suggests that the balance between too much and not enough Wnt signaling is a fine one, a concept that may be reflected in the relatively modest degree of rescue observed when we treated infected susceptible mice with recombinant DKK-1.

Constitutive activation of Wnt signaling constitutes the primary transforming event in colorectal cancer²⁹. Recent findings have highlighted a critical role for the R-spondins in colonic carcinogenesis¹⁸ but to our knowledge a role for R-spondins in susceptibility to enteric infections has never been described. Our findings also provide a potential hypothesis for how the response to specific commensal or pathogenic bacteria may participate in the development of colorectal cancer. Furthermore, our own analysis of the data from the 1st International Inflammatory Bowel Disease Genetics Consortium meta-analyses^{30,31} reveals strong associations of *RSPO3* with both Crohn's disease and ulcerative colitis (Supplementary Table S1–2), providing some evidence that R-spondins may have a broader role in linking infection or inflammation with intestinal homeostasis.

Mesenchymal-epithelial interactions orchestrate hedgehog (Hh), bone morphogenetic protein (Bmp), and Wnt signaling in the intestinal crypts and are critical for proper morphogenesis of intestinal architecture and for appropriate maintenance of the intestinal stem cell niche³². Mesenchymal cells of the intestinal lamina propria are also emerging as important players in immune function, and subepithelial myofibroblasts in particular are known to participate in innate³³ and adaptive immunity in the gut³⁴. Here we describe a new cross talk between the mesenchyme and the closely opposed epithelial compartment, critical for host tolerance against enteric pathogens, through R-Spondin 2 signaling. Our work illustrates a novel pathological pathway leading to fatal diarrhea and highlights a major role for intestinal mesenchyme in enteric infection outcome.

Lastly, while A/E pathogens still represent a clinical challenge with few therapeutic options, our work suggests that targeting the R-Spondin/Wnt signaling pathway could represent a new approach to treat A/E pathogen-induced diarrhea.

Methods

Mice

Breeding and experimental procedures were carried out in accordance with the Canadian Council on Animal Care and approved by our local ethical committee. C57BL/6J, C3H/HeOuJ, FVB/NJ and AKR/J mice were purchased from the Jackson Laboratory (Bar Harbor, ME, USA). All animals were maintained in a specific pathogen-free facility at McGill University. The congenic mice were produced according to standard procedures for introgression of C57BL/6J c15 allele onto the C3H/HeOuJ genome (C3Ou.B6-*Cri1*) or introgression of C3H/HeOuJ allele into C57BL/6J genome (B6.C3Ou-*Cri1*). Briefly, F1

mice were backcrossed to the parental strain. The resulting N2 mice with the desired segment of chr15 were selected by genotyping and used for subsequent backcrossing to the parental strain. Males and females (backcross generation N9) that inherited the intact derived congenic segment were intercrossed. Then, the offspring were genotyped to identify homozygotes for the desired segment, which were then intercrossed to maintain the line. To produce congenic sub-lines, F1 hybrids, made by crossing the congenic line to the recipient strain, were backcrossed to the recipient strain. Littermates issued from these backcrosses, characterized by recombination events within the *Cri1* locus, were selected by genotyping polymorphic SNP markers. The selected recombinant mice were then backcrossed again to the recipient strain. Males and female mice issued from this backcross (heterozygous for the reduced introgressed region) were intercrossed to fix the recombinant chromosome in the homozygous state. The *Cri-1* homozygous offspring were selected for brother-sister mating and foundation of the new congenic sub-lines.

Genotyping

DNA was extracted from biopsies of mouse tails with overnight digestion in lysis buffer and proteinase K, followed by a chloroform extraction. The complete list of genetic markers used for genotyping of congenic lines is included in Supplementary Table 1. In-house PCRs done for mouse genotyping were sent to Genome Quebec (Montreal, QC, Canada) for sequencing. PCR was performed using standard touchdown PCR methods with primers obtained from the Mouse Genome Informatics website (www.informatics.jax.org).

In vivo C. rodentium infection

Five-week-old male or female mice were inoculated with *C. rodentium* strain DBS100. Bacteria were grown overnight in 3 ml Luria-Bertani (LB) medium shaking at 37°C. Mice were infected by oral gavage of 0.1 ml of LB medium containing $2-3 \times 10^8$ CFUs of *C.rodentium*. The infectious dose was verified by plating of serial dilutions. For survival analysis, animals were monitored daily and moribund animals were euthanized by CO₂ when clinical endpoints were achieved¹³. Animals were euthanized on experimental days 3, 6, 9 or 13 and their colons isolated and processed for histological examination and immunostaining or snap-frozen for RNA/protein isolation. In some experiments, mice were daily iv. injected with human recombinant R-spondin 2 protein (250 µg.ml⁻¹ in PBS, R&D systems) from d3 to d5 after infection. For treatment with recombinant DKK1, mice were injected with DKK1 (iv. 25µg/day from d3 to d10 post infection and ip. 50µg/day from d11 to day 20). Production of recombinant DKK1 is described in Supplementary Methods.

Bone marrow chimeras

For bone marrow (BM) chimera experiments, recipient mice were lethally irradiated (950 rad/9.5 Gy) 24h before reconstitution with BM from the indicated donor line. BM was aseptically harvested from tibia and femur of the respective donor strain, and $5-10 \times 10^6$ cells were injected into the tail vein of the irradiated recipients. Mice received antibiotics (Baytril) in the drinking water during the following 2 weeks after bone marrow transfer and were allowed to reconstitute for a total of 8 weeks before being infected with *C. rodentium*. Chimerism 90% was validated by genotyping cell-sorted CD45+ splenocyte and tail DNA of chimeric mice with the polymorphic marker D15MIT229.

Histopathology and immunofluorescence

Distal colon sections were fixed in 10% buffered formalin, paraffin embedded, sectioned at 5 μm , and subsequently stained with hematoxylin and eosin (H&E) or Alcian blue (AB) using current procedures and visualized with a Zeiss axioscope microscope. Proliferative responses in infected tissues were scored in a blinded fashion by an expert veterinary pathologist. The average depth of 30 well-oriented colonic crypts was measured for each mouse. ImageJ software (Rasband, WS, ImageJ, rsb.info.nih.gov/ij) was used to quantify differences in Alcian blue staining between samples. To standardize measurements, all images were taken immediately after staining using identical camera settings.

Immunofluorescence was performed on paraffin sections. The slides were de-paraffinized with xylene twice for 5 minutes. The sections were rehydrated in ethanol 100% twice 5 minutes, followed by 90%, 70% ethanol and water, 5 minutes each. The slides were then incubated for 10 minutes in boiling 0.1 M citrate buffer (pH 6.0) for antigen retrieval. PBS 0.2 Tween 20 was used as wash buffer. After blocking in PBS 10% FCS 1% BSA for 1 hour at 37°C, tissues were incubated with primary antibodies against PCNA (Abcam, Cat #ab2426), β -catenin (BD, Cat# 610154), active β -catenin (Millipore, Cat# 05-665), CAR4 (R&D system, Cat# AF2414), at a dilution of 1:100 in PBS 1% BSA for 1 hour at 37°C. This step was followed by a 1 hour incubation with either Alexa-488 coupled goat anti rabbit, Alexa-488 coupled goat anti mouse, Alexa-488 coupled donkey anti goat respectively. Tissues were counterstained with 1:100 4',6'-diamidino-2-phenylindole (DAPI) for DNA staining (Sigma) and mounted using ProLong Gold Antifade reagent (Invitrogen). Sections were viewed on a Zeiss AxioImager microscope and images were obtained using a Zeiss AxioCam HRn camera operating through AxioVision software.

Quantitative real-time PCR

Mice were euthanized at indicated time points by CO₂ asphyxiation. The penultimate centimeter of colon was dissected and immediately snap frozen in liquid nitrogen. Samples were then stored at -80°C until processed. RNA from all tissue samples was isolated using Trizol reagent (Invitrogen, Carlsbad, CA) according to manufacturer's directions. Samples were DNase treated using TURBO Dnase (Ambion). cDNA was synthesized with SuperScript III Reverse Transcriptase (Invitrogen), using an Eppendorf PCR thermal cycler and random primers (Invitrogen). The purity of the samples was assessed spectrophotometrically; all samples had OD_{260/280} ratio between 1.8 and 2.0. Expression levels of the genes within *CriI* locus were assessed with TaqMan Gene Expression Assays (Applied Biosystems) on Applied Biosystems StepOne Plus Real-Time PCR system. For other genes, SYBR Green PCR reaction mix (10 μl) was composed of 5 μl LightCycler 480 SYBR Green I master (Roche), 4.5 μl of diluted cDNA, and a final concentration of 1 μM of each primer. Sequences of primers are in Supplementary Table S1. Primers were designed with sequences spanning exon-exon junctions or with a separation of at least one intron on the corresponding genomic DNA. Correct efficiency of primers was controlled by PCR reactions performed on serial dilutions of cDNA. PCR reactions were done using a Light Cycler 480 system (Roche).

Immunoblotting

Colonic tissues samples were homogenized in B150 lysis buffer (20 mM Tris-HCl pH 8.0, 150 mM KCl, 10% glycerol, 5 mM MgCl₂, and 0.1% NP40) supplemented with Complete-mini protease inhibitor (Roche). Equal protein aliquots were subjected to SDS-PAGE (10% acrylamide) under reducing condition and proteins were transferred to a 0.2 mm PVDF membrane (Bio-Rad). Blots were blocked with 5% skim milk overnight at 4°C, incubated with primary antibody against β -catenin (1:1000) (Cell Signaling, Cat# 9562), active β -catenin (Millipore, Cat# 05-665), CyclinD1 (Thermo Scientific, Cat# RM 9104) or β -actin (1:10,000) (Sigma, Cat# A 1978) for 1 hour at room temperature. Detections were done with appropriate horseradish peroxidase-conjugated secondary antibody and a chemiluminescent substrate (Millipore).

In Situ Hybridization

ISH was performed using ³⁵SUTP-labeled riboprobes synthesized in vitro from the *Rspo2* DNA template (NM_172815.3) with forward T7 primer: GCGCTATAATACGACTCACTATAGGGAGATAGCTCAGGCAGCGAGAACTTCA and reverse SP6: GCATTAATTTAGGTGACACTATAGAAGCGGCTGCAACCATTGTCCTTCGAACA. RNA probes were synthesized in vitro from a DNA template of 950 nts, antisense and sense with SP6 and T7 RNA polymerase activities, respectively and radiolabeled with ³⁵S-UTP (>1,000 Ci/mmol; Cat. #NEG039H, PerkinElmer LAS Canada, Inc.). 5 μ m FFPE sections were treated with Proteinase K (0.1 mg/ml) for 10–15 minutes. ³⁵S-labeled cRNA antisense and sense probes were used. Sections were hybridized overnight at 55°C in 50% deionized formamide, 0.3 M NaCl, 20 mM Tris- HCl, pH 7.4, 5 mM EDTA, 10 nM NaPO₄, 10% dextran sulfate, 1 x Denhardt's, subjected to stringent washing at 65°C in 50% formamide, 2 \times SSC, and 10 mM DTT, followed by washing in PBS before treatment with 20 μ g/ml RNase A at 37°C for 30 minutes. After washes in 2 \times SSC and 0.1 \times SSC for 10 minutes at 37°C, the slides were dehydrated, opposed to x-ray film for 5 days and then subjected to emulsion autoradiography. The autoradiography was revealed by treatment with D19 (Kodak) and sodium thiosulfate. We used frozen tissues cut into 6 μ m sections for the combined ISH and immunocytochemistry (ICC). Tissues were divided into 2 groups: first group with ICC and second group without ICC. In addition to fixation in 4% formaldehyde, both groups were treated with triethanolamine/acetic anhydride, washed and dehydrated with ethanol series and then submitted to a classical procedure. For subsequent ICC, tissue was treated with 3% H₂O₂ in water for 10 minutes to remove non-specific background, again washed with PBS and then pre-treated using heat-mediated antigen retrieval with sodium citrate buffer (pH=6) for 20 minutes. Primary antibodies anti Gr-1 (Ebioscience, Cat #14-5931-81) and anti α -SMA (Abcam, Cat #ab5694) were diluted 1:100 in 1% BSA/PBS and incubated overnight at 4°C. Immunoreaction was revealed using anti-rabbit- (or anti-rat) biotinylated second antibody (1:250) followed by HRP (Vector). The staining appears brown under lightfield illumination. Tissue was then lightly stained with cresyl violet and mounted under cover slips.

Statistics

Statistic differences between pairs of survival curves of mice grouped by genotype were calculated using log-rank tests. Gene expression data were analyzed by the Mann-Whitney test. *, $P < 0.05$; **, $P < 0.01$; ***, $P < 0.001$

Supplementary Material

Refer to Web version on PubMed Central for supplementary material.

Acknowledgments

This work was supported by a CIHR Operating Grant awarded to SG (MOP-89817). ST and AT were supported by CIHR studentships. ED was supported by a Fellowship from CIHR/Canadian Association of Gastroenterology. SG is a Canada Research Chair. We thank Rusty Jones and Jorg Fritz (McGill University) for helpful discussions for the bone marrow chimera experiments.

References

1. Chen HD, Frankel G. Enteropathogenic *Escherichia coli*: unravelling pathogenesis. *FEMS Microbiol Rev.* 2005; 29:83–98. [PubMed: 15652977]
2. Nataro JP, Kaper JB. Diarrheagenic *Escherichia coli*. *Clin Microbiol Rev.* 1998; 11:142–201. [PubMed: 9457432]
3. McDaniel TK, Jarvis KG, Donnenberg MS, Kaper JB. A genetic locus of enterocyte effacement conserved among diverse enterobacterial pathogens. *Proc Natl Acad Sci U S A.* 1995; 92:1664–1668. [PubMed: 7878036]
4. Wales AD, Woodward MJ, Pearson GR. Attaching-effacing bacteria in animals. *J Comp Pathol.* 2005; 132:1–26. [PubMed: 15629476]
5. Fagundes-Neto U, Kallas MR, Patricio FR. Morphometric study of the small bowel mucosa in infants with diarrhea due to enteropathogenic *Escherichia coli* strains. *Hepatogastroenterology.* 1997; 44:1051–1056. [PubMed: 9261598]
6. Karch H. The role of virulence factors in enterohemorrhagic *Escherichia coli* (EHEC)--associated hemolytic-uremic syndrome. *Semin Thromb Hemost.* 2001; 27:207–213. [PubMed: 11446654]
7. Mundy R, MacDonald TT, Dougan G, Frankel G, Wiles S. *Citrobacter rodentium* of mice and man. *Cell Microbiol.* 2005; 7:1697–1706. [PubMed: 16309456]
8. Barthold SW, Osbaldiston GW, Jonas AM. Dietary, bacterial, and host genetic interactions in the pathogenesis of transmissible murine colonic hyperplasia. *Lab Anim Sci.* 1977; 27:938–945. [PubMed: 599885]
9. Vallance BA, Deng W, Jacobson K, Finlay BB. Host susceptibility to the attaching and effacing bacterial pathogen *Citrobacter rodentium*. *Infect Immun.* 2003; 71:3443–3453. [PubMed: 12761129]
10. Borenshtein D, Nambiar PR, Groff EB, Fox JG, Schauer DB. Development of fatal colitis in FVB mice infected with *Citrobacter rodentium*. *Infect Immun.* 2007; 75:3271–3281. [PubMed: 17470543]
11. Borenshtein D, et al. Diarrhea as a cause of mortality in a mouse model of infectious colitis. *Genome Biol.* 2008; 9:R122. [PubMed: 18680595]
12. Borenshtein D, et al. Decreased expression of colonic *Slc26a3* and carbonic anhydrase iv as a cause of fatal infectious diarrhea in mice. *Infect Immun.* 2009; 77:3639–3650. [PubMed: 19546193]
13. Diez E, et al. Identification and characterization of *Cri1*, a locus controlling mortality during *Citrobacter rodentium* infection in mice. *Genes Immun.* 2011; 12:280–290. [PubMed: 21326319]
14. Teatero SA, et al. The *Cri1* locus is the common genetic cause of susceptibility to *Citrobacter rodentium* infection in C3H and FVB mouse strains. *Gut Microbes.* 2011; 2:173–177. [PubMed: 21804358]

15. Kim KA, et al. R-Spondin proteins: a novel link to beta-catenin activation. *Cell Cycle*. 2006; 5:23–26. [PubMed: 16357527]
16. Kim KA, et al. Mitogenic influence of human R-spondin1 on the intestinal epithelium. *Science*. 2005; 309:1256–1259. [PubMed: 16109882]
17. de Lau W, et al. Lgr5 homologues associate with Wnt receptors and mediate R-spondin signalling. *Nature*. 2011; 476:293–297. [PubMed: 21727895]
18. Seshagiri S, et al. Recurrent R-spondin fusions in colon cancer. *Nature*. 2012; 488:660–664. [PubMed: 22895193]
19. van de Wetering M, et al. The beta-catenin/TCF-4 complex imposes a crypt progenitor phenotype on colorectal cancer cells. *Cell*. 2002; 111:241–250. [PubMed: 12408868]
20. van den Brink GR, et al. Indian Hedgehog is an antagonist of Wnt signaling in colonic epithelial cell differentiation. *Nat Genet*. 2004; 36:277–282. [PubMed: 14770182]
21. Byeon MK, et al. The down-regulated in adenoma (DRA) gene encodes an intestine-specific membrane glycoprotein. *Oncogene*. 1996; 12:387–396. [PubMed: 8570216]
22. Schweinfest CW, Henderson KW, Suster S, Kondoh N, Papas TS. Identification of a colon mucosa gene that is down-regulated in colon adenomas and adenocarcinomas. *Proc Natl Acad Sci U S A*. 1993; 90:4166–4170. [PubMed: 7683425]
23. Kato A, Romero MF. Regulation of electroneutral NaCl absorption by the small intestine. *Annu Rev Physiol*. 2011; 73:261–281. [PubMed: 21054167]
24. Hoglund P, et al. Mutations of the Down-regulated in adenoma (DRA) gene cause congenital chloride diarrhoea. *Nat Genet*. 1996; 14:316–319. [PubMed: 8896562]
25. Schweinfest CW, et al. slc26a3 (dra)-deficient mice display chloride-losing diarrhea, enhanced colonic proliferation, and distinct up-regulation of ion transporters in the colon. *J Biol Chem*. 2006; 281:37962–37971. [PubMed: 17001077]
26. Brandl K, Beutler B. Creating diseases to understand what prevents them: genetic analysis of inflammation in the gastrointestinal tract. *Curr Opin Immunol*. 2012; 24:678–685. [PubMed: 23123276]
27. Gruenheid S, Gros P. Forward genetic dissection of innate response to infection in inbred mouse strains: selected success stories. *Clin Exp Immunol*. 2010; 162:393–401. [PubMed: 21070206]
28. Kuhnert F, et al. Essential requirement for Wnt signaling in proliferation of adult small intestine and colon revealed by adenoviral expression of Dickkopf- 1. *Proc Natl Acad Sci U S A*. 2004; 101:266–271. [PubMed: 14695885]
29. Barker N, et al. Crypt stem cells as the cells-of-origin of intestinal cancer. *Nature*. 2009; 457:608–611. [PubMed: 19092804]
30. Anderson CA, et al. Meta-analysis identifies 29 additional ulcerative colitis risk loci, increasing the number of confirmed associations to 47. *Nat Genet*. 2011; 43:246–252. [PubMed: 21297633]
31. Franke A, et al. Genome-wide meta-analysis increases to 71 the number of confirmed Crohn's disease susceptibility loci. *Nat Genet*. 2010; 42:1118–1125. [PubMed: 21102463]
32. Powell DW, Pinchuk IV, Saada JI, Chen X, Mifflin RC. Mesenchymal cells of the intestinal lamina propria. *Annu Rev Physiol*. 2011; 73:213–237. [PubMed: 21054163]
33. Pang G, Couch L, Batey R, Clancy R, Cripps A. GM-CSF, IL-1 alpha, IL-1 beta, IL-6, IL-8, IL-10, ICAM-1 and VCAM-1 gene expression and cytokine production in human duodenal fibroblasts stimulated with lipopolysaccharide, IL-1 alpha and TNF-alpha. *Clin Exp Immunol*. 1994; 96:437–443. [PubMed: 8004813]
34. Roberts AI, Nadler SC, Ebert EC. Mesenchymal cells stimulate human intestinal intraepithelial lymphocytes. *Gastroenterology*. 1997; 113:144–150. [PubMed: 9207272]

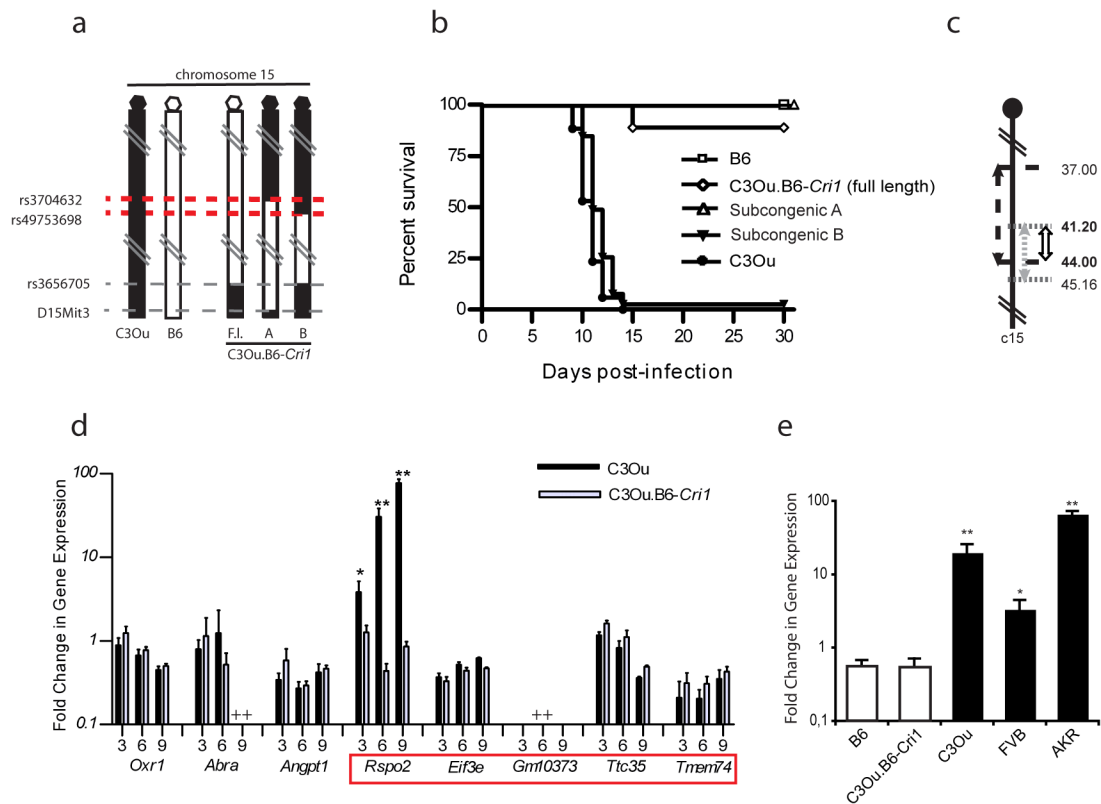


Figure 1. Positional cloning of the *Cri1* locus and identification of the *Rspo2* gene as a major candidate gene for susceptibility to *C. rodentium* infection

(a) Genetic map of congenic and subcongenic C3Ou.B6-*Cri1* mice. Black indicates regions from C3Ou genome and white indicate regions from B6 genome. (b) Survival of B6, C3Ou, congenic and subcongenic C3Ou.B6-*Cri1* mice following oral infection with *C. rodentium*. C3Ou.B6-*Cri1* (diamonds) and subcongenic A mice (open triangles) show high levels of resistance, whereas subcongenic B mice (filled triangles) are nearly completely susceptible. These results pinpoint *Cri1* localization to an interval between marker rs3704632 and marker rs49753698 ($n > 15$). (c) Mapping of *Cri1* by linkage analysis (black dotted arrow) and genetic dissection using subcongenic mice (grey dotted arrow) restrict the candidate region (white arrow) (d) Expression of all genes within the candidate region was assayed by qPCR in whole colon tissues on C3Ou and C3Ou.B6-*Cri1* left untreated or at indicated time after infection; results are expressed as the expression fold variation in infected mice versus untreated littermates ($n = 4$) at day 3, 6, and 9 post infection. (e) *Rspo2* expression in B6, C3Ou, C3Ou.B6-*Cri1*, AKR and FVB mice ($n = 6$) after 6 days of infection with *C. rodentium*. Data are representative of three experiments. Error bars in histograms represent s.e.m. *, $P < 0.05$; **, $P < 0.01$ (Mann-Whitney test) here and for all figures. Statistical differences between pairs of survival curves of mice grouped by genotype were calculated using logrank test. *** $p < 0.0001$

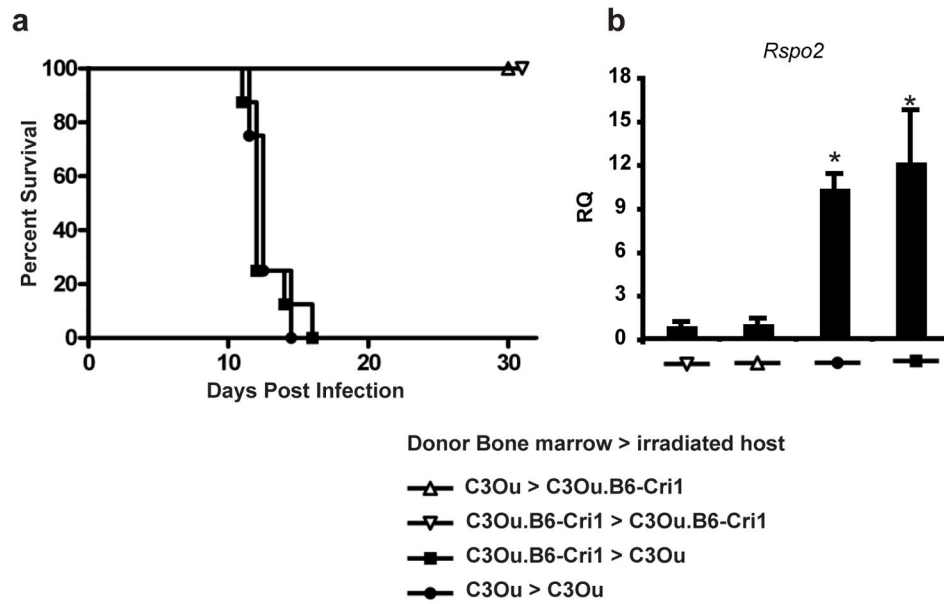


Figure 2. *Cri1* mediated susceptibility to *C. rodentium* infection and colonic expression of *Rspo2* are controlled by radio-resistant cells

(a) Survival curve of reciprocal bone marrow chimera mice infected with *C. rodentium* demonstrate that susceptibility to infection is independent of bone marrow transferred cells but depends on the genotype of the irradiated host (n>4). (a) Relative quantification (RQ) of *Rspo2* expression assessed by qPCR in colonic tissues from reciprocal bone marrow chimeric mice at 7 days post infection with *C. rodentium* (n=4). Data represent one of two experiments.

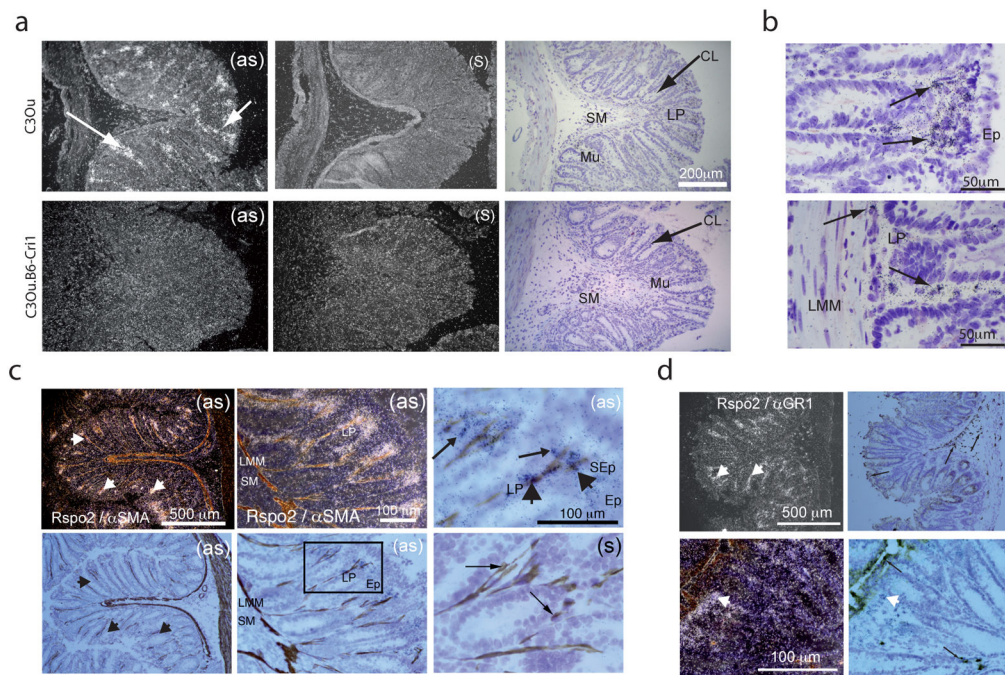


Figure 3. *Cri1* controls *C. rodentium*-induced *Rspo2* expression within the colonic lamina propria
(a) Emulsion autoradiography detection of *Rspo2* mRNA antisense labeling (as) by in situ hybridization (ISH) or control (s) hybridization in the colon mucosa seen as bright under darkfield illumination in susceptible C3Ou or resistant C3Ou.B6-Cri1 at 6 days post infection. Signal was detected in the microscopical loci seen in the bottom (large arrow) and close to luminal pole (small arrow) of the lamina propria; the same sections with cresyl violet staining (right). **(b)** Enlarged view of *Rspo2* positive cells in infected susceptible C3Ou mice, ISH labeling (arrow) is observed in the Lamina Propria, close to the colonic epithelia (top) and at the bottom of the gland (bottom). **(c)** Comparative localization of *Rspo2* mRNA and α SMA in the colon of susceptible C3Ou mice 7 days post infection, seen at various magnification levels under darkfield (top left, top middle) or brightfield illumination (bottom left, bottom middle). Middle bottom panel is an enlargement of the boxed area in the top right panel. Far right panel is a control with sense labeling. Large arrowheads indicate double *Rspo2* and α SMA labeling. Also observed are single-labeled *Rspo2* mRNA+ cells found along the LP axis and in the subepithelial region (small arrow). **(d)** Comparative localization of *Rspo2* mRNA and Gr1 in the colon of susceptible C3Ou mice 7 days post infection, seen at various magnification levels under darkfield or brightfield illumination. Large arrows indicate *Rspo2* positive cells and thin arrows indicate Gr1 positive cells mostly in subepithelial regions, in the lamina muscularis mucosae and in the sub mucosae (thin arrows). Data are representative of three independent experiments. Abbreviations: CL - Crypts of Lieberkühn; SM - Sub-Mucosae; Mu – Mucosae ; LMM – Lamina Muscularis Mucosae; LP – Lamina Propria ; SEP - sub-epithelial region; Ep - Epithelia

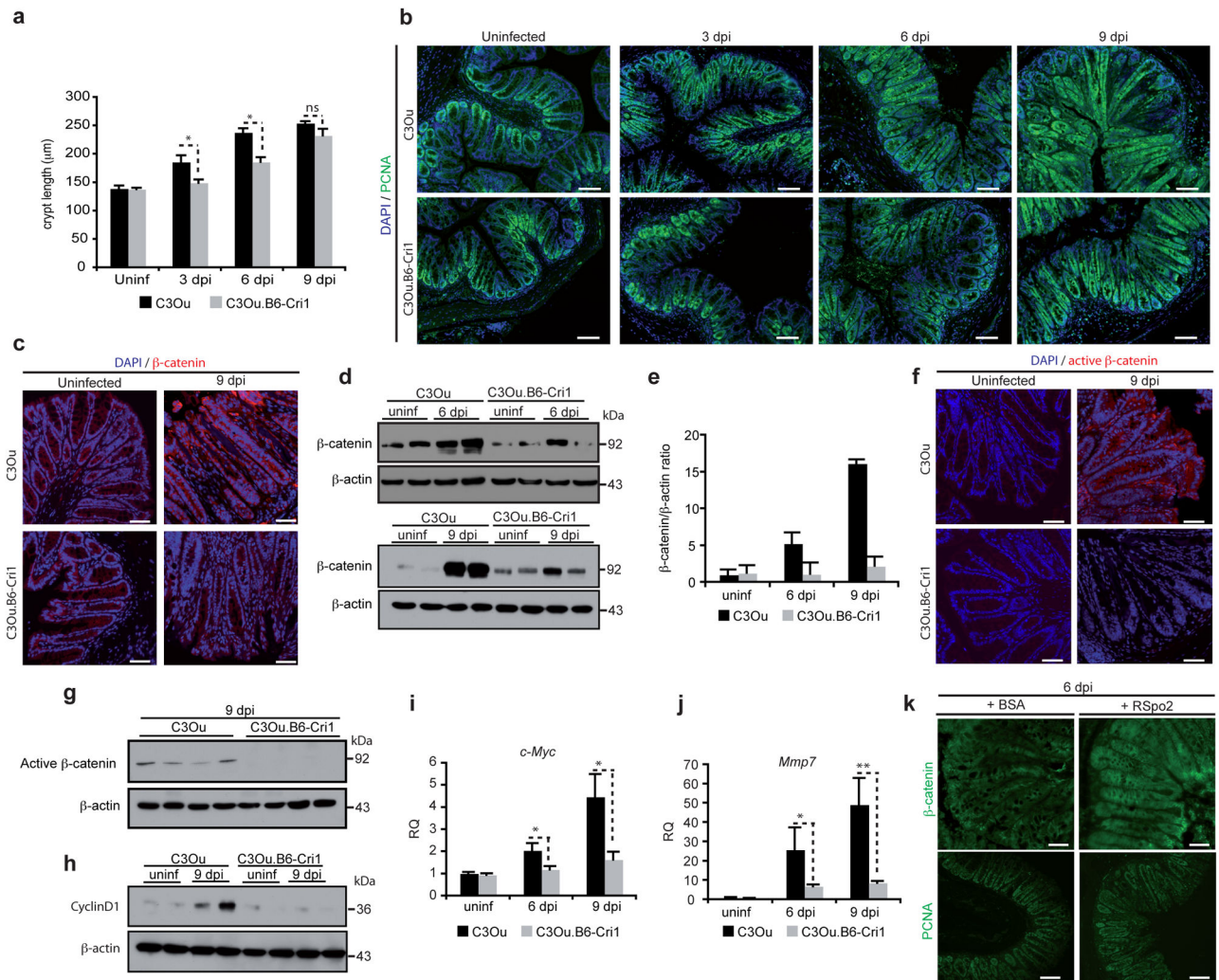


Figure 4. *Cri1* controls crypt hyperplasia and canonical Wnt signaling activation during *C. rodentium* infection

(a) Crypt length measurements in the distal colon of C3Ou (black bars) or C3Ou.B6-*Cri1* congenic mice (grey bars) left uninfected or at indicated time after infection (dpi: day post infection). (b) PCNA immuno-stained (green)/DAPI co-stained (blue) colon sections of C3Ou or C3Ou.B6-*Cri1* mice at indicated time points after infection (scale bar: 100µm). (c) β -catenin immuno-stained (red)/DAPI co-stained (blue) colon sections of C3Ou or C3Ou.B6-*Cri1* mice left untreated or 9 days after *C. rodentium* infection. Exposure times were the same for each sample and were optimized to avoid signal saturation in the C3Ou sample (scale bar: 50 µm). (d) Lysates of distal colon samples were assayed for β -catenin levels by immunoblotting. (e) Densitometry analysis of (d). (f–g) Immunodetection of dephosphorylated active β -catenin by immunofluorescence (f) or western blotting (g) in C3Ou or C3Ou.B6-*Cri1* mice (scale bar: 50 µm). In (f), exposure times were the same for each sample and were optimized to avoid signal saturation in the C3Ou sample. Immunoblot of CyclinD1 (h) and relative quantification by qPCR analysis of *c-Myc* and *Mmp7* expression (i–j) in C3Ou or C3Ou.B6-*Cri1* mice (n>6). Data are representative of three

independent experiments. **(k)** Recombinant R-spondin 2 (RSpo2) treatment induces epithelial proliferation and β -catenin activation. Representative images of β -catenin (top) (scale bar: 50 μ m) and PCNA (bottom) (scale bar: 100 μ m) stained colon sections of resistant C3Ou.B6-*Cri1* congenic mice, at 6 days after infection treated with recombinant RSpo2 or BSA. C3Ou.B6-*Cri1* were daily iv. injected with hRSpo2 or equal amount of BSA from d3 to d5 after infection (d3, 4: 50 μ g; d5: 100 μ g). (n=6) Data are representative of two independent experiments.

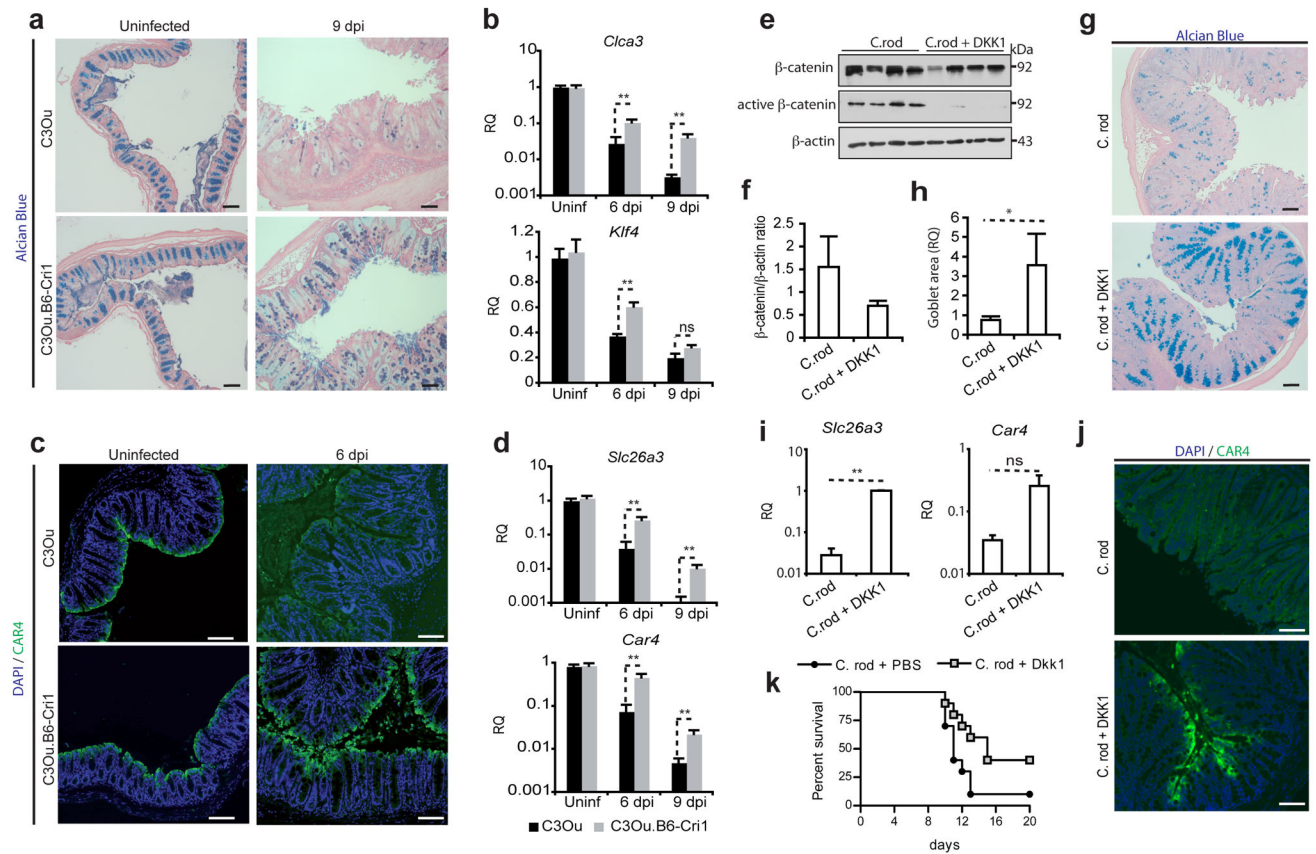


Figure 5. *Cri1* controls loss of epithelial differentiation during *C. rodentium* infection
Cri1 controls level of goblet cell (a–b) and mature enterocyte (c–d) loss during *C. rodentium* infection. (a) FFPE colon sections from C3Ou and C3Ou.B6-*Cri1* stained with Alcian blue (which stains mature goblet cells) (20× magnification). (scale bar: 100 μm). (b) qPCR analysis of the goblet cell markers *Clca3* and *Klf4* in C3Ou versus C3Ou.B6-*Cri1* mice (n=6). (c) Immuno-detection of CAR4 expression in enterocytes from C3Ou or C3Ou.B6-*Cri1* mice (scale bar: 100 μm). (d) qPCR analysis of *Slc26a3* and *Car4* expression in C3Ou and C3Ou.B6-*Cri1* mice at various time points after infection (n=6). Data are representative of three independent experiments. (e–h) DKK1 treatment inhibits β-catenin activation and loss of epithelial differentiation during *C. rodentium* infection. Susceptible C3Ou mice were infected with *C. rodentium* and daily iv. injected with recombinant DKK1 (C. rod + DKK1) or with PBS (C. rod) starting at day three post infection. (e) Lysates of distal colon samples were assayed for β-catenin levels by immunoblotting at day 7 post infection. (f) Densitometry analysis of (e). Alcian blue staining (g) and automatic quantification of level of intensity of Alcian blue staining (h) carried out with ImageJ software in sections of infected C3Ou mice, PBS or DKK1-treated at day 7 post infection (n=5) (scale bar: 100 μm). (i) Relative quantification by qPCR analysis of *Slc26a3* and *Car4* expression and immunostaining of CAR4 (j) in DKK1 treated mice and PBS control mice at day 7 post infection (n=5) (scale bar: 100 μm). (k) Survival curve of C3Ou mice infected with *C. rodentium* and treated with DKK1 or with PBS (n=10) Data are representative of two independent experiments.

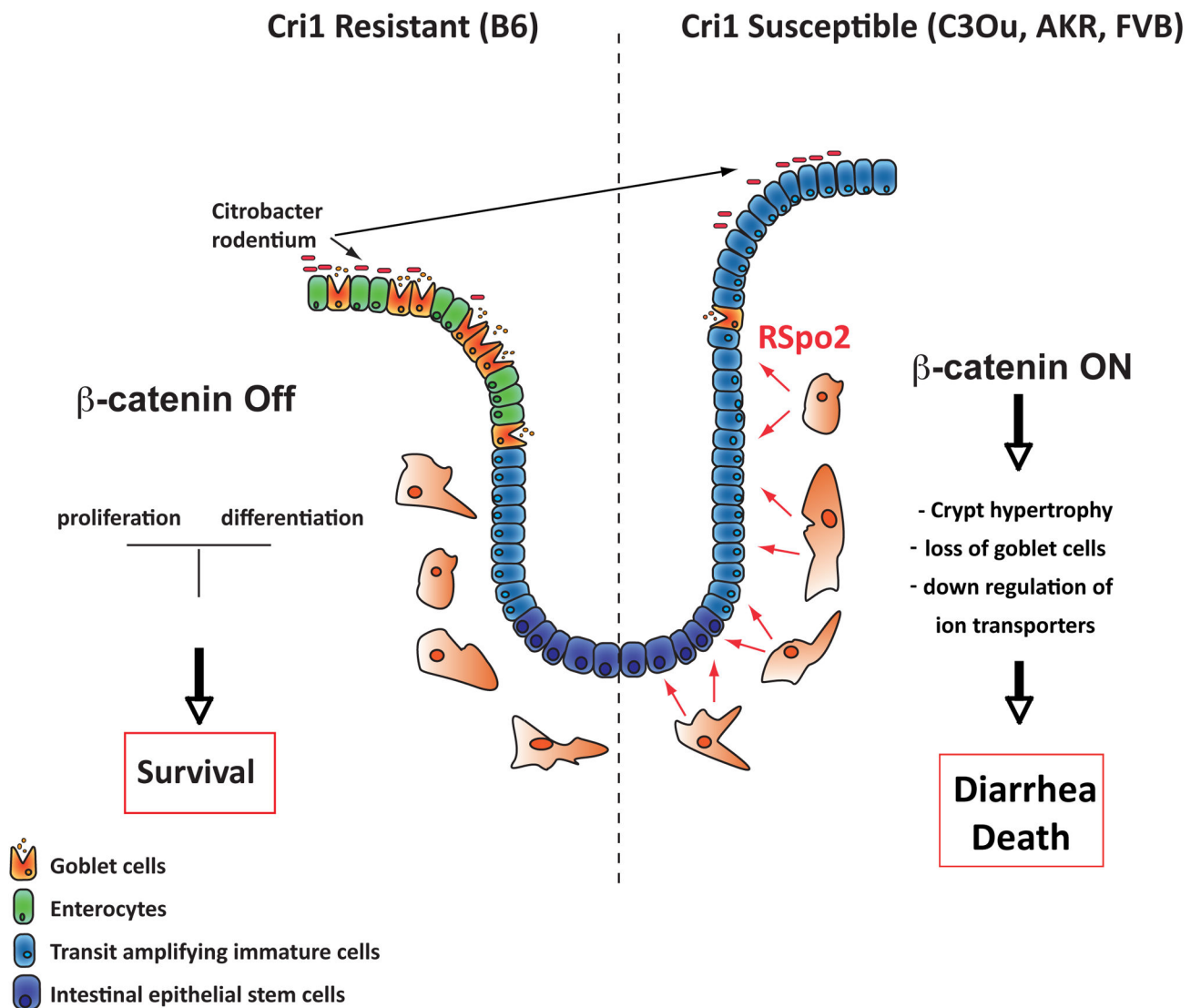


Figure 6. A model for susceptibility to *C. rodentium* infection

Following infection, *Rspo2* is expressed in the colonic mucosa of susceptible mice. R-spondin 2 (*Rspo2*) triggers Wnt-pathway activation in transit-amplifying cells and leads to proliferation of immature precursors together with an inhibition in the differentiation of mature enterocytes and goblet cells. The resulting undifferentiated epithelium is no longer able to provide vital functions for fluid absorption, leading to lethal diarrhea.